Available online at www.sciencedirect.com
SCIENCE DIRECT®
Nuclear Instruments and Methods in Physics Research B 249 (2006) 752–755
NIM B
Beam Interactions with Materials & Atoms
www.elsevier.com/locate/nimb

Ion transmission through nano-apertures

M.L. Taylor [a], R.D. Franich [a,*], A. Alves [a], P. Reichart [b], D.N. Jamieson [b], P.N. Johnston [a]

[a] Applied Physics, RMIT University, GPO Box 2476V, Melbourne, Vic. 3001, Australia
[b] Microanalytical Research Centre, School of Physics, University of Melbourne, Vic. 3010, Australia

Available online 19 May 2006

Abstract

Localisation of ion impacts with a resolution better than can be achieved with a focused ion beam microprobe may potentially be achieved by employing a high-aspect ratio nano-aperture mask. The present paper applies Monte Carlo methods to investigate the role of ion scattering and straggling through the aperture and the influence of these processes on the transmitted ion energy and intensity distribution. The objective of the investigation is to determine the potential of this method for delivering few or single ions to sub-100 nm locations on substrates. Simulation of 2 and 4 MeV He, 8 MeV F and 71 MeV Cu has indicated that the masking process is effective, with probabilities between 82% and 93% of obtaining single ions with full energy at the exit of the aperture. Possible applications include precision ion doping, single-ion machining and potentially ion beam analysis.

PACS: 07.05.Tp; 02.70.Uu; 61.18.Bn; 81.16.Nd

Keywords: Ion beam analysis; Ion beam lithography; High aspect ratio structures; Nuclear microprobe; Monte Carlo modelling; Nano-stencil

1. Introduction

Applications for ion beams requiring the precision delivery of few or single ions to high resolution are emerging [1–3]. There are two main methods for the delivery of ions to sub-100 nm resolution: focusing by means of electric or magnetic lenses or by collimation with apertures. For MeV ions, focusing is generally preferred because of the difficulty of making high aspect ratio apertures required, however focusing ions to sub-100 nm beam spots entails considerable technical complexity [4]. With the advent of methods for making sub-100 nm high aspect ratio apertures [5–8], we investigate the trajectories of ions emerging from such apertures with the goal of ultimately exploiting the trail of latent damage induced by the passage of a single ion, typically 20 nm in diameter. Ion scattering and straggling through the walls of the aperture and the fact that all materials are partially transparent to MeV ions will limit the spatial resolution for the delivery of ions regardless of the diameter of the aperture itself.

These phenomena can be modelled with a Monte Carlo (MC) ion transport simulation which is a useful technique for studying problems in which individual ion histories are relevant, or where the treatment of the ion beam as a continuous distribution is inappropriate. The passage of ions through a sample with a complex geometry such as an aperture is an example of such a problem and can be investigated with MC simulation.

2. Monte Carlo simulation

The MC approach involves modelling the interaction of the beam with the sample by explicitly calculating individual ion trajectories. A fast FORTRAN ion transport simulation code based on the TRIM code [9] has been adapted to the problem of ions passing through a high aspect-ratio aperture used as a collimator. The code is described in

* Corresponding author. Tel.: +61 3 9925 9555; fax: +61 3 9925 5290.
E-mail address: rick.franich@rmit.edu.au (R.D. Franich).

0168-583X/$ - see front matter © 2006 Elsevier B.V. All rights reserved.
doi:10.1016/j.nimb.2006.03.132

detail in [10,11], however, the recoil specific efficiency enhancements are not employed here. The code has been modified to model an aperture in a mask which has a thickness that exceeds the ion beam range by considering the aperture as a cylindrical void in the mask. The original code modelled ion transport in a 2-D projection for efficiency reasons. The present code models the ion transport in 3-D which is required to model individual ion paths which intersect the aperture.

Ions that enter the aperture are transported, without electronic energy loss or nuclear scattering, to the point at which the trajectory intersects with the aperture wall or is transmitted beyond the mask. The points of intersection of the trajectory and the aperture wall are determined by equating and solving the parametric equations for a cylinder and a line of any free flight segment which enters the aperture.

As the sample is not laterally homogeneous, the ion positions relative to the aperture are tracked explicitly and ions may be made incident at any point relative to the aperture, with an incident angle consistent with the ion beam that delivers the ions to the mask.

The ions of primary interest are the fraction which are not transmitted directly through the aperture, but have a trajectory that intersects the aperture wall, or are incident upon the mask near the aperture and subsequently scatter into the aperture so that they are transmitted through the mask albeit with reduced energy. The net effect will be a beam broadening at the aperture exit analogous to the penumbra seen in radiotherapy and optical collimation of non-point sources.

3. Model and experimental configuration

Nano-scale apertures have been drilled by focused ion beam systems in silicon cantilevers. These structures are attractive for use as a nano-stencil [12] potentially allowing sub-1 nm control of the position of the aperture in the cantilever above the substrate as well as precision mapping of location markers on the substrate by scanning probe microscopy. SEM images of apertures in silicon cantilevers show a radius of the order of 100 nm can be achieved. We therefore apply our model to high-aspect ratio apertures in silicon masks.

We apply the MC simulation to various ion-energy combinations and model the mask as a uniform Si layer with a 100 nm radius cylindrical aperture through a slab whose thickness is chosen to be approximately twice the range of the incident ions used in each case. We also consider some alternatives for beam energy and aperture size to demonstrate their effects on the transmission spectra. In practice, we consider that the ion beam is delivered onto the mask by a focused ion beam system, such as a nuclear microprobe, where the beam spot will be much larger than the aperture. For our simulations the beam is modelled with a one micrometer radius. To obtain insights into the influence of ion energy, mass and range we have run simulations for 2 MeV He, 8 MeV F and 71 MeV Cu ions, for which

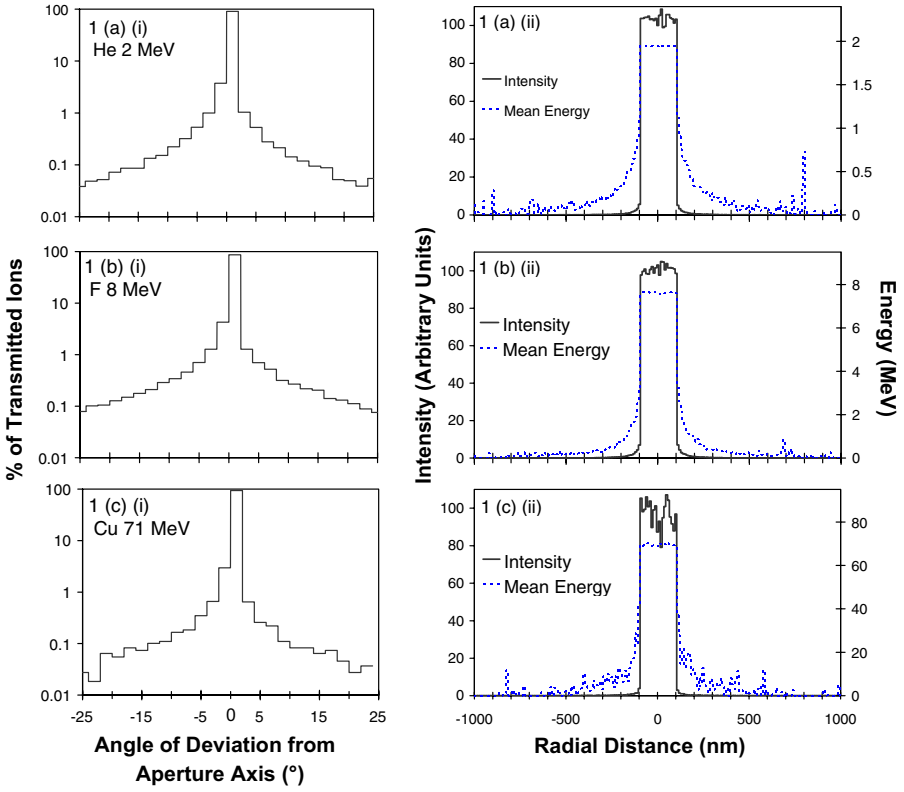

Fig. 1. Transmission of (a – i,ii) 2 MeV He, (b – i,ii) 8 MeV F and (c – i,ii) 71 MeV Cu through a 100 nm radius nano-aperture.

experimental data will be available in the near future [5]. In our simulations, 10^7 incident ions were modelled in each case except for 71 MeV Cu which used 10^6 ions due to the much longer simulation times associated with heavy ions.

4. Results

For each transmitted ion, the simulation calculates the energy, position and direction cosines at the point of exit from the mask. Fig. 1 shows the spatial distribution and mean energy of transmitted ions as a function of radial distance from the centre of the aperture. The distribution of transmission angles from the sample normal is also shown.

Table 1
Ion-energy systems: percent of ions transmitted with full energy, T, percent of transmitted ions scattered out of the aperture, S_{out}, scattered into the aperture, S_{in}, and the mean energy of the latter ions, $\overline{E}_{in}$

Ion/Energy (MeV)	Aperture radius (nm)	T (%)	S_{out} (%)	S_{in} (%)	$\overline{E}_{in}$ (MeV)
He/2	100	86.44	3.51	10.05	0.990
F/8	100	82.22	4.54	13.24	3.240
Cu/71	100	90.26	2.15	7.59	31.582
He/2	40	92.79	2.42	4.79	1.015
He/4	100	89.84	3.16	7.00	2.110

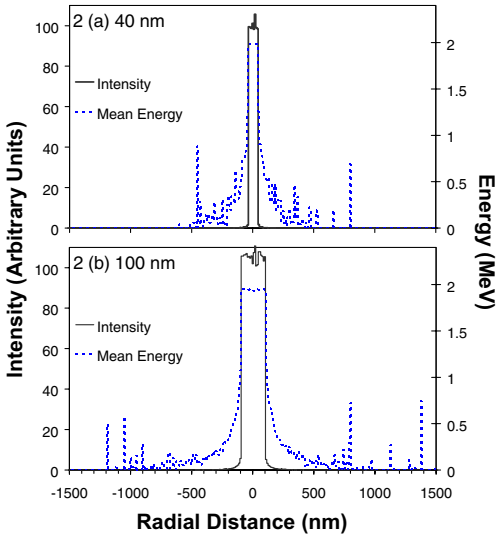

Fig. 2. Transmission of 2 MeV He ions through (a) 40 nm and (b) 100 nm radii nano-apertures.

For single ion applications, the radial intensity plot should be interpreted as a probability distribution. The mean energy per ion represents the expected transmission energy, as a function of position.

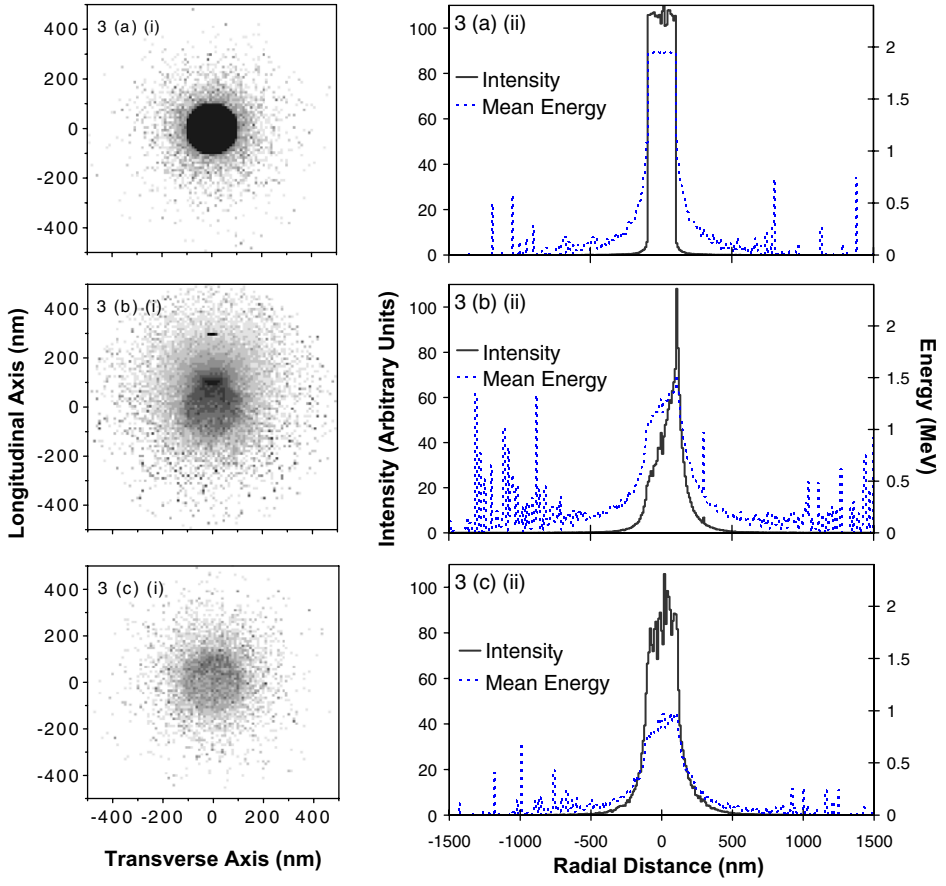

Fig. 3. Transmission of 2 MeV He ions through a nano-aperture of 100 nm in radius at three incident angles (a) normal (b) $\theta_c/2$ and (c) θ_c (see text).

The percentage of transmitted ions which exit the aperture while retaining their full energy is denoted by T. Of all transmitted ions, a fraction, S_{out}, are scattered out of the aperture, and S_{in} are scattered in to the aperture spot with reduced energy. The mean energy of these inwardly scattered ions is $\overline{E}_{in}$. The remaining fraction are those that pass freely through the aperture. Table 1 summarises these quantities for each ion-energy-aperture system.

For a one micron radius ion beam centred on a 100 nm radius aperture (1% of the beam area), the total percentage of ions transmitted is 1.15%, 1.22% and 1.09% for He, F and Cu, respectively. These numbers are greater than 1% due to scattering in the walls of the aperture. From the data in Fig. 1((a)–(c))(i), it is evident that the great majority of ions are transmitted along the axis of the beam, with scattering of 8 MeV F resulting in the greatest distribution of exit angles. The conspicuous features of the energy distributions are the few high energy counts far from the aperture. These are single ion strikes following large angle scattering in the mask. While these are the counts that contribute the greatest deviations from the intended location of the ions, they are extremely rare events. Of the 10^7 incident 2 MeV He ions, there are 79 beyond the tailing region at four aperture radii with $E > 100$ keV; compared to 111,481 within the aperture radius, i.e. only 0.07% of the transmitted ions. Although the tailing is narrower, this scattering effect is somewhat more pronounced for smaller apertures. For the 40 nm aperture of Fig. 2, the number of counts outside four radii and $E > 100$ keV is 59 compared to 16,596 counts within the spot, i.e. 0.36%.

Ions which enter the mask at an angle to the normal are expected to undergo more significant scattering. In Fig. 3 we illustrate the scattering distribution for three different incident angles. The mask 'closure angle', θ_c, is chosen as a characteristic angle of the system – the angle at which the path length through edges of the aperture becomes equal to the ion range. Plots corresponding to ions of normal incidence and half θ_c are also presented. The simulations in Fig. 3 show the skewing of the transmission spot, and the broadening of the scattered distributions illustrates the importance of the alignment between the beam and aperture axis. The reduction of the peak energy at greater angles verifies the experimental alignment technique of tilting the sample until the energy peak is a maximum.

5. Conclusion

Monte Carlo simulation is a very successful technique for evaluation of experimental systems and parameters, for specific outcomes or tolerances. The distributions for various ion-energy combinations are very similar and systems may be scaleable for appropriate choices of ion, energy, aperture size and mask thickness. The intensity distributions show that the masking process works well – the steep intensity at the aperture edge coupled with sharp energy reduction are the desired features for single ion lithography. Exploitation of these characteristics enables tailoring of lithographic processes where there exists a threshold damage density below which etching does not occur. Future work involves comparison with the SCATT technique employed by Adamczewski et al. [13], and further experimental investigation.

References

[1] T. Schenkel, A. Persaud, S.J. Park, J. Nilsson, J. Bokor, J.A. Liddle, R. Keller, D.H. Schneider, D.W. Cheng, D.E. Humphries, J. Appl. Phys. 94 (2003) 7017.
[2] T. Schenkel, A. Persaud, S.J. Park, J. Meijer, J.R. Kingsley, J.W. MacDonald, J.P. Holder, J. Bokor, D.H. Schneider, J. Vac. Sci. Tech. B 20 (2002) 2819.
[3] T. Schenkel, J. Meijer, A. Persaud, J.W. MacDonald, J.P. Holder, D.H. Schneider, SPIE Proc. San Jose (USA) 4656 (January) (2002) 10.
[4] A. Alves, S.M. Hearne, P. Reichart, R. Siegele, D.N. Jamieson, P.N. Johnston, Ion beam lithography with single ions, SPIE Proc. 5650 (2005) 381.
[5] A. Alves, P. Reichart, R. Siegele, P.N. Johnston, D.N. Jamieson, Nucl. Instr. and Meth. B, these Proceedings, doi:10.1016/j.nimb.2006.03.128.
[6] P. Grabiec, J. Radojewski, M. Zaborowski, K. Domanski, T. Schenkel, I.W. Rangelow, J. Vac. Sci. Tech. B 22 (2004) 16.
[7] C. Lehrer, L. Frey, S. Peterson, Th. Sulzbach, O. Ohlsson, Th. Dziomba, H.U. Danzebrink, H. Russel, Microelectron. Eng. 57–58 (2001) 721.
[8] Th. Dziomba, Th. Sulzbach, O. Ohlsson, C. Lehrer, L. Frey, H.U. Danzebrink, SXM-3 Proc. 5–6 (1999) 486.
[9] J.P. Biersack, U. Littmark, The Stopping and Range of Ions in Solids, Pergamon, New York, 1985.
[10] R.D. Franich, P.N. Johnston, I.F. Bubb, N. Dytlewski, D.D. Cohen, Nucl. Instr. and Meth. B 190 (2002) 252.
[11] R.D. Franich, P.N. Johnston, I.F. Bubb, Nucl. Instr. and Meth. B 219–220 (2004) 87.
[12] R. Luthi, R.R. Schittler, J. Brugger, P. Vettiger, M.E. Welland, J.K. Gimzewski, App. Phys. Lett. 75 (1999) 1314.
[13] J. Adamczewski, J. Meijer, A. Stephan, H.H. Bukow, C. Rolfs, Nucl. Instr. and Meth. B 114 (1996) 172.